EUROPEAN ORGANIZATION FOR NUCLEAR RESEARCH


CERN-PPE/92-152
16 September 1992

# High Mass Photon Pairs in $\ell^+\ell^-\gamma\gamma$ Events at LEP

The L3 Collaboration

## Abstract

From the analysis of the reactions

$$e^+e^- \to \ell^+\ell^-(n\gamma) \quad (\ell = e, \mu, \tau)$$

we observe four events, one $e^+e^-\gamma\gamma$ and three $\mu^+\mu^-\gamma\gamma$, with the invariant mass of the photon pairs close to 60 GeV. These events were selected from a data sample collected in the L3 detector corresponding to 950,000 produced $Z^0$'s. More data are necessary to ascertain the origin of these events.

(Submitted to *Physics Letters B*)

# Introduction

We report the results from the analysis of the following reactions:

$$e^+e^- \to \ell^+\ell^-(n\gamma) \quad (\ell = e, \mu, \tau) \, .$$

Four $\ell^+\ell^-\gamma\gamma$ ($\ell = e, \mu$) events were seen with an invariant mass of the two isolated photons close to 60 GeV in the data collected from the 1990 and 1991 runs as well as 1992 run through July 15, corresponding to a total integrated luminosity of 27 pb$^{-1}$ and a sample of 950,000 $Z^0$'s produced at center-of-mass energies ranging from 88.2 to 93.8 GeV.

The L3 detector [1] is especially designed to detect and precisely measure electrons, muons and photons. During the construction and operation of the L3 detector, much effort has been spent to ensure that the design resolution is maintained. Analysis of the data from $Z^0$ decays in the last three years of running has shown that, indeed, we have obtained the design resolution [2]:

$$\frac{\Delta E}{E} \leq 2.0\% \quad \text{for } E > 1.5 \quad \text{GeV}$$

for electrons and photons, and

$$\frac{\Delta p}{p} = 2.5\% \quad \text{at } p = 45 \quad \text{GeV}$$

for muons. The angular resolution for electrons, muons, and photons is better than 0.2°. The good resolution for photons enabled us to study one-photon [3] and two-photon [4] final state events.

The data recorded in the following polar angle ranges are used in the analysis:

| | |
|---|---|
| time expansion chamber (TEC): | $25° \leq \theta \leq 155°$, |
| electromagnetic calorimeter (BGO): | $11° \leq \theta \leq 169°$, |
| hadron calorimeter: | $5° \leq \theta \leq 175°$, |
| muon spectrometer: | $36° \leq \theta \leq 144°$, |

where $\theta$ is defined with respect to the beam axis. For the analysis of $\mu^+\mu^-(n\gamma)$ events, the full data sample is used while only the data collected in 1991 and 1992 corresponding to an integrated luminosity of 21 pb$^{-1}$ are used in $e^+e^-(n\gamma)$ and $\tau^+\tau^-(n\gamma)$ analysis.

The first two events (one in 1990 and the other in 1991) have $M_{\gamma\gamma} = 58.8$ GeV ($M_{\mu\mu} = 27.1$ GeV) and $M_{\gamma\gamma} = 59.0$ GeV ($M_{\mu\mu} = 25.3$ GeV). In 1992 two more events were observed, one with $M_{\gamma\gamma} = 62.0$ GeV ($M_{\mu\mu} = 20.0$ GeV) and the other with $M_{\gamma\gamma} = 60.0$ GeV ($M_{ee} = 17.9$ GeV). Figs. 1a-1d show these four events. The measured properties of the events are summarized in Table 1.

Radiation from initial and final state leptons is the expected source for hard and isolated photon production. The process is well described by Quantum Electrodynamics (QED) and, in principle, can be accurately simulated by Monte Carlo programs.

We first describe the selection criteria for $\ell^+\ell^-(n\gamma)$ events. To understand the origin of these events, we compare the observed kinematic distributions with those expected from QED Monte Carlo simulation and discuss the possible excess of events with high mass photon pairs.

| **Event 1** | $\mu^+$ | $\mu^-$ | $\gamma$ | $\gamma$ |
|---|---|---|---|---|
| E (GeV) | 10.5 | 20.7 | 35.9 | 24.6 |
| $\theta$ (deg) | 96.7 | 69.2 | 113.1 | 71.2 |
| $\phi$ (deg) | 131.3 | 357.0 | 175.9 | 337.8 |
| Pair Mass | $M_{\mu\mu} = 27.1 \pm 1.4$ GeV | | $M_{\gamma\gamma} = 58.8 \pm 0.6$ GeV | |
| | | | | |
| **Event 2** | $\mu^+$ | $\mu^-$ | $\gamma$ | $\gamma$ |
| E (GeV) | 12.7 | 16.9 | 33.1 | 28.1 |
| $\theta$ (deg) | 81.7 | 130.0 | 46.3 | 117.1 |
| $\phi$ (deg) | 301.7 | 179.4 | 136.1 | 345.2 |
| Pair Mass | $M_{\mu\mu} = 25.3 \pm 0.4$ GeV | | $M_{\gamma\gamma} = 59.0 \pm 0.6$ GeV | |
| | | | | |
| **Event 3** | $\mu^+$ | $\mu^-$ | $\gamma$ | $\gamma$ |
| E (GeV) | 11.9 | 15.2 | 39.1 | 25.1 |
| $\theta$ (deg) | 98.1 | 115.4 | 66.9 | 106.8 |
| $\phi$ (deg) | 66.7 | 326.1 | 164.8 | 328.2 |
| Pair Mass | $M_{\mu\mu} = 20.0 \pm 0.4$ GeV | | $M_{\gamma\gamma} = 62.0 \pm 0.6$ GeV | |
| | | | | |
| **Event 4** | $e^+$ | $e^-$ | $\gamma$ | $\gamma$ |
| E (GeV) | 3.4 | 24.4 | 42.0 | 21.6 |
| $\theta$ (deg) | 103.6 | 62.1 | 109.6 | 80.4 |
| $\phi$ (deg) | 102.7 | 268.5 | 92.6 | 278.9 |
| Pair Mass | $M_{ee} = 17.9 \pm 0.2$ GeV | | $M_{\gamma\gamma} = 60.0 \pm 0.6$ GeV | |

Table 1: The measured properties of the four events with high mass photon pairs. The center-of-mass energies ($\sqrt{s}$) of these events are 91.23, 91.26, 91.25 and 91.36 GeV respectively.

# Event Selection

We first describe the identification of photons and leptons, followed by the selection of $\ell^+\ell^-(n\gamma)$ events.

A cluster with energy deposited in BGO calorimeter greater than 0.5 GeV is accepted as an electromagnetic cluster if $E_9/E_{25} > 0.9$ or $E_2/E_9 > 0.7$. $E_9$ and $E_{25}$ are the energies deposited in the $3 \times 3$ and $5 \times 5$ crystal arrays centered around the most energetic crystal. $E_2$ is the energy deposited in the two most energetic crystals. Electromagnetic clusters with energy greater than 1.0 GeV and within the fiducial volume defined by $|\cos\theta| < 0.9$ are considered for photon selection. $\theta$ is the polar angle of the cluster with respect to the beam axis. Clusters with energy greater than 3.0 GeV and within the fiducial volume defined by $|\cos\theta| < 0.74$ are considered for electron selection.

We now consider $\Delta\phi$, the angle in the $R-\phi$ plane between the centroid of electromagnetic cluster and the nearest TEC track which has at least 10 $R-\phi$ hits, a distance of closest approach to the interaction point in the $R-\phi$ plane of less than 10 mm, and a transverse momentum greater than 100 MeV. Clusters which satisfy $|\Delta\phi| < 20$ mrad are selected as electron candidates while those which fail this criterion are selected as photon candidates.

Muons are identified and measured in the muon chamber system. We require that a muon track consists of track segments in at least two of the three layers of the muon chambers, as well as a transverse distance of closest approach and a longitudinal distance of closest approach to the interaction point of less than 100 mm each. In addition, the identified muon is required to have a momentum greater than 3.0 GeV.

Taus are identified by their distinct one- and three-prong decays. Neighboring TEC tracks within 20° in the $R-\phi$ plane are grouped together and then matched with calorimetric clusters to form tau candidates. The candidates must be in the fiducial volume defined by $|\cos\theta| < 0.74$. To remove background from multihadronic events, each tau candidate is required to have between one and three good TEC tracks. A good track has at least 30 $R-\phi$ hits, a distance of closest approach less than 5.0 mm, and a transverse momentum greater than 100 MeV. In addition, the total visible energy in a cone of 15° half-opening angle with respect to the jet direction is required to be greater than 3.0 GeV. To suppress electrons and muons arising from $e^+e^- \to e^+e^-(n\gamma), \mu^+\mu^-(n\gamma)$ processes, the sum of the electromagnetic and muon energy in each tau candidate is required to be less than $0.4\sqrt{s}$.

We now consider the selection of $\ell^+\ell^-(n\gamma)$ events. These events are characterized by low cluster and track multiplicity. Clusters are constructed from calorimetric hits. Only clusters with an energy greater than 100 MeV are considered. To suppress hadronic background, $e^+e^-(n\gamma)$ and $\mu^+\mu^-(n\gamma)$ candidates are required to have less than 12 clusters. For $\tau^+\tau^-(n\gamma)$ candidates, the number of clusters is required to be less than 20.

Events which have two electrons and total electromagnetic energy greater than $0.6\sqrt{s}$ are selected as $e^+e^-(n\gamma)$ events.

Events with two muons are considered as $\mu^+\mu^-(n\gamma)$ candidates. To reject background from two-photon processes and $\tau^+\tau^-(n\gamma)$, the sum of the electromagnetic energy and the momenta of muon tracks is required to be greater than $0.6\sqrt{s}$. To remove cosmic ray events, we require at least one good TEC track. Events with exactly one good TEC track are further required to have at least one scintillator hit within 3.0 ns of the beam crossing.

Events with two identified taus with an opening angle in the $R-\phi$ plane of at least 30° are considered as $\tau^+\tau^-(n\gamma)$ candidates. To reject events from two-photon processes, the energy of at least one tau is required to exceed $0.1\sqrt{s}$ and the polar angle of the direction of missing momentum is required to be at least 25.8° with respect to the beam axis. The background events from $e^+e^-(n\gamma)$ and $\mu^+\mu^-(n\gamma)$ are suppressed by requiring the sum of the electromagnetic and muon energy in the event to be less than $0.8\sqrt{s}$.

We now study events which contain isolated photons in addition. These photons are required to be at least 8° away from electrons, 5° from muons, and 15° from taus. Tighter photon isolation requirement for the $e^+e^-(n\gamma)$ events is to reject overlapping electromagnetic showers and for the $\tau^+\tau^-(n\gamma)$ events to reduce backgrounds from the $\pi^0$'s. The total number of selected events in each channel are shown in Table 2.

# Comparison with QED Predictions

To compare the measured distributions with the expectations from QED, we use the Monte Carlo program YFS3 as described in Ref. [5]. The program generates events of the type $e^+e^- \to \mu^+\mu^-(n\gamma)$ according to the Yennie-Frautschi-Suura scheme [6] with multiple collinear and soft photon radiation in both the initial and final states. It includes the additional leading-log terms for one or two hard photons. The cross section for the production of events with hard

and isolated photons as calculated by the program has been found to be in good agreement with the exact $\mathcal{O}(\alpha^2)$ matrix element calculations [7].

The program is adequate to describe the $e^+e^- \to \tau^+\tau^-(n\gamma)$ process since only photons with energies greater than 1.0 GeV and opening angles with respect to the nearest tau direction greater than 15° are considered, so that tau mass effects are negligible. The t-channel contribution to $e^+e^- \to e^+e^-(n\gamma)$ process is not modeled by YFS3 Monte Carlo program. Instead we use the pure s-channel distributions for comparisons with $e^+e^-(n\gamma)$ data.

To determine the acceptance for $\ell^+\ell^-$ events with photons in the final state, 150,000 Monte Carlo $e^+e^- \to \mu^+\mu^-(n\gamma)$ events, generated at a center-of-mass energy of 91.2 GeV, are subjected to the full L3 detector simulation [8]. The simulated events are then reconstructed and analyzed with the same program as that used for the data. A total of 84,633 Monte Carlo events are selected after the $\mu^+\mu^-(n\gamma)$ selection criteria described above are applied. The number of expected $\mu^+\mu^-$ events with one or more photons from QED is then given by:

$$N_\gamma^{exp} = R_\gamma \cdot N_{\mu\mu}^D$$

where $N_{\mu\mu}^D$ is the total number of selected $\mu^+\mu^-(n\gamma)$ events in the data and $R_\gamma$ is the fraction of events with one or more photons in the Monte Carlo sample after event selection. The numbers of expected $e^+e^-$ and $\tau^+\tau^-$ events with photons are calculated in the same way, except that the ratio $R_\gamma$ is rescaled according to the different acceptances calculated from the generator level Monte Carlo sample for the different angle requirements between photons and leptons.

The effect from the enhanced initial state radiation for the data above the $Z^0$ peak is found to be small since only 3% of the accepted events in the data come from center-of-mass energies 2.0 GeV or more above the $Z^0$ peak. Table 2 shows the expected numbers of $\ell^+\ell^-$ events in the data as well as the expectations from the Monte Carlo. The statistical error on the expected number of events from the Monte Carlo is 1.1% for one or more and 6.0% for two or more photons. For the comparison described below, the contributions from all three lepton flavours are added together.

| number | Data | | | | MC Expectations | | | |
|---|---|---|---|---|---|---|---|---|
| of photons | $e^+e^-$ | $\mu^+\mu^-$ | $\tau^+\tau^-$ | $\ell^+\ell^-$ | $e^+e^-$ | $\mu^+\mu^-$ | $\tau^+\tau^-$ | $\ell^+\ell^-$ |
| $n \geq 0$ | 19068 | 17548 | 11971 | 48587 | — | — | — | — |
| $n \geq 1$ | 1370 | 1377 | 617 | 3364 | 1306 | 1386 | 630 | 3322 |
| $n \geq 2$ | 55 | 68 | 16 | 139 | 45 | 56 | 17 | 118 |

Table 2: Numbers of $\ell^+\ell^-(n\gamma)$ events in the data together with the expected numbers from the Monte Carlo. The numbers of Monte Carlo events are normalized to the corresponding numbers of data events with $n \geq 0$.

The energy distribution of the most energetic photon for events with one or more photons in the final state is compared with the prediction of YFS3 Monte Carlo program in Fig. 2a. Fig. 2b shows the energy spectrum of the second most energetic photon for events with at least two photons. Fig. 3 shows the comparison with the Monte Carlo for the angle between the most energetic photon and the nearest charged lepton for events with one or more photons. The Monte Carlo distributions in the above figures are obtained from a high statistics sample corresponding to approximately $10^7$ $e^+e^- \to \mu^+\mu^-(n\gamma)$ events. These are generator level events selected with criteria similar to those used for the $\ell^+\ell^-(n\gamma)$ events in the data. The distributions

are normalized to the expected number of events obtained from the fully simulated Monte Carlo events shown in Table 2.

Monte Carlo studies at the generator level show that the energy spectra are not sensitive to variations in the isolation requirements between leptons and photons. The possible distortion of the energy and angle spectra due to the energy and angular dependence of the acceptance has been investigated using the fully simulated $\mu^+\mu^-(n\gamma)$ events. No significant effect is observed. As shown in the figures, the predicted Monte Carlo distributions for events with one or more photons are in good agreement with the data in both the shape and the normalization.

# High Mass Photon Pair Events

In this section, we discuss the characteristics of the events with at least two photons in the final state, as selected by the above procedure. For events with more than two photons, the highest invariant mass of any combination is taken as $M_{\gamma\gamma}$. Figs. 4a and 4b show the two dimensional scatter plot of $M_{\gamma\gamma}$ versus $M_{\ell\ell}$ for the data and for the Monte Carlo after detector simulation respectively, where $M_{\ell\ell}$ is the invariant mass of the lepton pair for $e^+e^-$ and $\mu^+\mu^-$ events, and the recoiling mass of the photon pair for $\tau^+\tau^-$ events. Among 139 data events with at least two photons (fig. 4a), four events have the invariant mass of the photon pair clustering around 60 GeV and are well separated from the other events. Three are $\mu^+\mu^-\gamma\gamma$ events and the fourth is an $e^+e^-\gamma\gamma$ event.

The two dimensional distribution of $M_{\gamma\gamma}$ versus $\cos\theta_{\gamma\ell}$ is shown in Fig. 5a for the data and in Fig. 5b for the fully simulated Monte Carlo events, where $\theta_{\gamma\ell}$ is defined as the smallest angle in the event between any lepton and photon. Most of the events shown in the figures have small values of $\theta_{\gamma\ell}$ and $M_{\gamma\gamma}$, characteristic of QED radiation. We note that $\theta_{\gamma\ell}$ is small and that the sum of the energies of the lepton and the nearest photon is close to the beam energy for three of the four events with high mass photon pairs.

Fig. 6 shows the $M_{\gamma\gamma}$ distribution compared with the prediction of the Monte Carlo program. The Monte Carlo distribution is obtained from the same high statistics $e^+e^- \rightarrow \mu^+\mu^-(n\gamma)$ sample used for Figs. 2 and 3 and normalized in the same manner. It can be seen that the Monte Carlo underestimates the number of data events with two or more photons in the final state.

QED does not predict clustering of $M_{\gamma\gamma}$ around 60 GeV and we determine the probability for observing four or more events around 60 GeV from QED fluctuation in our data. We simulate $10^6$ experiments with the average number of events in each experiment equal to the total number of events (139) in the $M_{\gamma\gamma}$ distribution of the data. The shape of the $M_{\gamma\gamma}$ distribution is obtained from the shape of the predicted Monte Carlo distribution shown in Fig. 6. The instances of events clustering within a single mass bin of $\Delta M_{\gamma\gamma} = \pm 2.5$ GeV are counted. This bin width corresponds to eight times the $M_{\gamma\gamma}$ measurement error at 60 GeV. The probability for observing four or more clustered events, all with $M_{\gamma\gamma} > 50$ GeV, is found to be $\mathcal{O}(10^{-3})$.

Events of the type $e^+e^- \rightarrow \nu\bar{\nu}\gamma\gamma$ have also been searched for in the data collected from 1991 and 1992 runs, applying similar requirements on the photons and requiring the polar angle of the direction of missing momentum to be greater than 25.8° with respect to the beam axis. No event is found with $M_{\gamma\gamma} > 10$ GeV. It should also be noted that, with different isolation criteria and in a data sample of approximately 450,000 $Z^0$'s corresponding to an integrated luminosity of 13 $pb^{-1}$, no hadronic event containing isolated photon pair with $M_{\gamma\gamma} > 40$ GeV has been observed in our data [9].

# Conclusions

In a sample of events corresponding to 950,000 produced $Z^0$'s, we observe one $e^+e^-\gamma\gamma$ and three $\mu^+\mu^-\gamma\gamma$ events with an invariant mass of the photon pair close to 60 GeV. These photons could arise from the decay of a massive particle. However, the probability for all four events originating from QED is estimated to be $\mathcal{O}(10^{-3})$. Therefore, a QED fluctuation cannot be ruled out. More data are necessary to ascertain the origin of these events.

# Acknowledgments

We would like to thank S. Jadach, B.F.L. Ward and Z. Wąs for providing us the YFS3 Monte Carlo program used in this analysis. We wish to express our gratitude to the CERN accelerator divisions for the excellent performance of the LEP machine. We acknowledge the contributions of all the engineers and technicians who have participated in the construction and maintenance of this experiment.

## The L3 Collaboration:


O.Adriani[14] M.Aguilar-Benitez[23] S.Ahlen[9] J.Alcaraz[15] A.Aloisio[26] G.Alverson[10] M.G.Alviggi[26] G.Ambrosi[31] Q.An[16] H.Anderhub[45] A.L.Anderson[13] V.P.Andreev[35] L.Antonov[39] D.Antreasyan[7] P.Arce[23] A.Arefiev[25] A.Atamanchuk[35] T.Azemoon[3] T.Aziz[1,8] P.V.K.S.Baba[16] P.Bagnaia[34] J.A.Bakken[33] L.Baksay[41] R.C.Ball[3] S.Banerjee[8] J.Bao[5] R.Barillère[15] L.Barone[34] A.Baschirotto[24] R.Battiston[31] A.Bay[17] F.Becattini[14] U.Becker[13,45] F.Behner[45] J.Behrens[45] Gy.L.Bencze[11] J.Berdugo[23] P.Berges[13] B.Bertucci[31] B.L.Betev[39,45] M.Biasini[31] A.Biland[45] G.M.Bilei[31] R.Bizzarri[34] J.J.Blaising[4] G.J.Bobbink[15,2] R.Bock[1] A.Böhm[1] B.Borgia[34] M.Boseti[24] D.Bourilkov[28] M.Bourquin[17] D.Boutigny[4] B.Bouwens[2] E.Brambilla[26] J.G.Branson[36] I.C.Brock[32] M.Brooks[21] A.Bujak[42] J.D.Burger[13] W.J.Burger[17] J.Busenitz[41] X.D.Cai[16] M.Capell[20] M.Caria[31] G.Carlino[26] A.M.Cartacci[14] R.Castello[24] M.Cerrada[23] F.Cesaroni[34] Y.H.Chang[13] U.K.Chaturvedi[16] M.Chemarin[22] A.Chen[47] C.Chen[6] G.M.Chen[6] H.F.Chen[18] H.S.Chen[6] M.Chen[13] W.Y.Chen[47] G.Chiefari[26] C.Y.Chien[5] M.T.Choi[40] S.Chung[13] C.Civinini[14] I.Clare[13] R.Clare[13] T.E.Coan[21] H.O.Cohn[29] G.Coignet[4] N.Colino[15] A.Contin[7] X.T.Cui[16] X.Y.Cui[16] T.S.Dai[13] R.D'Alessandro[14] R.de Asmundis[26] A.Degré[4] K.Deiters[43] E.Dénes[11] P.Denes[33] F.DeNotaristefani[34] M.Dhina[45] D.DiBitonto[41] M.Diemoz[34] H.R.Dimitrov[39] C.Dionisi[34,15] L.Djambazov[45] M.T.Dova[16] E.Drago[26] T.Driever[28] D.Duchesneau[17] P.Duinker[2] I.Duran[37] S.Easo[31] H.El Mamouni[22] A.Engler[32] F.J.Eppling[13] F.C.Erné[2] P.Extermann[17] R.Fabbretti[43] M.Fabre[43] S.Falciano[34] S.J.Fan[38] O.Fackler[20] J.Fay[22] M.Felcini[15] T.Ferguson[32] D.Fernandez[23] G.Fernandez[23] F.Ferroni[34] H.Fesefeldt[1] E.Fiandrini[31] J.Field[17] F.Filthaut[28] G.Finocchiaro[34] P.H.Fisher[5] G.Forconi[17] T.Foreman[2] K.Freudenreich[45] W.Friebel[44] M.Fukushima[13] M.Gailloud[19] Yu.Galaktionov[25,13] E.Gallo[14] S.N.Ganguli[15,8] P.Garcia-Abia[23] D.Gele[22] S.Gentile[34,15] S.Goldfarb[10] Z.F.Gong[18] E.Gonzalez[23] A.Gougas[5] D.Goujon[17] G.Gratta[30] M.Gruenewald[30] C.Gu[16] M.Guanziroli[16] J.K.Guo[38] V.K.Gupta[33] A.Gurtu[8] H.R.Gustafson[3] L.J.Gutay[42] K.Hangarter[1] A.Hasan[16] D.Hauschildt[2] C.F.He[38] J.T.He[6] T.Hebbeker[1] M.Hebert[36] G.Herten[13] A.Hervé[15] K.Hilgers[1] H.Hofer[45] H.Hoorani[17] G.Hu[16] G.Q.Hu[38] B.Ille[22] M.M.Ilyas[16] V.Innocente[15] H.Janssen[15] S. Jezequel[4] B.N.Jin[6] A.Kasser[19] R.A.Khan[16] Yu.Kamyshkov[29] P.Kapinos[35,44] J.S.Kapustinsky[21] Y.Karyotakis[15] M.Kaur[16] S.Khokhar[16] M.N.Kienzle-Focacci[17] J.K.Kim[40] S.C.Kim[40] Y.G.Kim[40] W.W.Kinnison[21] D.Kirkby[30] S.Kirsch[44] W.Kittel[28] A.Klimentov[13,25] A.C.König[28] E.Koffeman[2] O.Kornadt[1] V.Koutsenko[13,25] A.Koulbardis[35] R.W.Kraemer[32] T.Kramer[13] V.R.Krastev[39,31] W.Krenz[1] A.Krivshich[35] H.Kuijten[28] K.S.Kumar[12] A.Kunin[12,25] G.Landi[14] D.Lanske[1] S.Lanzano[26] P.Lebrun[22] P.Lecomte[45] P.Lecoq[15] P.Le Coultre[45] D.M.Lee[21] I.Leedom[10] C.Leggett[3] J.M.Le Goff[15] R.Leiste[44] M.Lenti[14] E.Leonardi[34] X.Leytens[2] C.Li[18,16] H.T.Li[6] P.J.Li[38] X.G.Li[6] J.Y.Liao[38] W.T.Lin[47] Z.Y.Lin[18] F.L.Linde[15] B.Lindemann[1] L.Lista[26] Y.Liu[16] W.Lohmann[44,15] E.Longo[34] Y.S.Lu[6] J.M.Lubbers[15] K.Lübelsmeyer[1] C.Luci[34] D.Luckey[7,13] L.Ludovici[34] L.Luminari[34] W.Lustermann[44] W.G.Ma[18] M.MacDermott[45] P.K.Malhotra[8†] R.Malik[16] A.Malinin[25] C.Maña[23] M.Maolinbay[45] P.Marchesini[45] F.Marion[4] A.Marin[9] J.P.Martin[22] L.Martinez-Laso[23] F.Marzano[34] G.G.G.Massaro[2] K.Mazumdar[8] P.McBride[12] T.McMahon[42] D.McNally[45] M.Merk[32] L.Merola[26] M.Meschini[14] W.J.Metzger[28] Y.Mi[19] G.B.Mills[21] Y.Mir[16] G.Mirabelli[34] J.Mnich[1] M.Möller[1] B.Monteleoni[14] R.Morand[4] S.Morganti[34] N.E.Moulai[16] R.Mount[30] S.Müller[1] A.Nadtochy[35] E.Nagy[11] M.Napolitano[26] H.Newman[30] C.Neyer[45] M.A.Niaz[16] A.Nippe[1] H.Nowak[44] G.Organtini[34] D.Pandoulas[1] S.Paoletti[14] P.Paolucci[26] G.Pascala[34] G.Passaleva[14,31] S.Patricelli[26] T.Paul[5] M.Pauluzzi[31] C.Paus[1] F.Pauss[45] Y.J.Pei[1] S.Pensotti[24] D.Perret-Gallix[4] J.Perrier[17] A.Pevsner[5] D.Piccolo[26] M.Pieri[15] P.A.Piroué[33] F.Plasil[29] V.Plyaskin[25] M.Pohl[45] V.Pojidaev[25,14] H.Postema[13] Z.D.Qi[38] J.M.Qian[3] K.N.Qureshi[16] R.Raghavan[8] G.Rahal-Callot[45] P.G.Rancoita[24] M.Rattaggi[24] G.Raven[2] P.Razis[27] K.Read[29] D.Ren[45] Z.Ren[16] M.Rescigno[34] S.Reucroft[10] A.Ricker[1] S.Riemann[44] W.Riemers[42] O.Rind[3] H.A.Rizvi[16] F.J.Rodriguez[23] M.Röhner[1] S.Röhner[1] L.Romero[23] J.Rose[1] S.Rosier-Lees[4] R.Rosmalen[28] Ph.Rosselet[19] A.Rubbia[13] J.A.Rubio[15] H.Rykaczewski[45] M.Sachwitz[44] E.Sajan[31] J.Salicio[15] J.M.Salicio[23] G.S.Sanders[21] A.Santocchia[31] M.S.Sarakinos[13] G.Sartorelli[7,16] M.Sassowsky[1] G.Sauvage[4] V.Schegelsky[35] D.Schmitz[1] P.Schmitz[1] M.Schneegans[4] H.Schopper[46] D.J.Schotanus[28] S.Shotkin[13] H.J.Schreiber[44] J.Shukla[32] R.Schulte[1] S.Schulte[1] K.Schultze[1] J.Schwenke[1] G.Schwering[1] C.Sciacca[26] I.Scott[12] R.Sehgal[16] P.G.Seiler[43] J.C.Sens[15,2] L.Servoli[31] I.Sheer[36] D.Z.Shen[38] S.Shevchenko[30] X.R.Shi[30] E.Shumilov[25] V.Shoutko[25] D.Son[40] A.Sopczak[36] C.Spartiotis[5] T.Spickermann[1] P.Spillantini[14] R.Starosta[1] M.Steuer[7,13] D.P.Stickland[33] F.Sticozzi[13] H.Stone[17] K.Strauch[12] B.C.Stringfellow[42] K.Sudhakar[8] G.Sultanov[16] L.Z.Sun[18,16] H.Suter[45] J.D.Swain[16] A.A.Syed[28] X.W.Tang[6] L.Taylor[10] G.Terzi[24] Samuel C.C.Ting[13] S.M.Ting[13] M.Tonutti[1] S.C.Tonwar[8] J.Tóth[11] A.Tsaregorodtsev[35] G.Tsipolitis[32] C.Tully[30] K.L.Tung[6] J.Ulbricht[45] L.Urbán[11] U.Uwer[1] E.Valente[34] R.T.Van de Walle[28] I.Vetlitsky[25] G.Viertel[45] P.Vikas[16] U.Vikas[16] M.Vivargent[4] H.Vogel[32] H.Vogt[44] I.Vorobiev[25] A.A.Vorobyov[35] L.Vuilleumier[19] M.Wadhwa[4,16] W.Wallraff[1] C.Wang[13] C.R.Wang[18] G.H.Wang[32] X.L.Wang[18] Y.F.Wang[13] Z.M.Wang[16,18] A.Weber[1] J.Weber[45] R.Weill[19] T.J.Wenaus[20] J.Wenninger[17] M.White[13] C.Willmott[23] F.Wittgenstein[15] D.Wright[33] S.X.Wu[16] B.Wysłouch[13] Y.Y.Xie[38] J.G.Xu[6] Z.Z.Xu[18] Z.L.Xue[38] D.S.Yan[38] B.Z.Yang[18] C.G.Yang[6] G.Yang[16] C.H.Ye[16] J.B.Ye[18] Q.Ye[16] S.C.Yeh[47] Z.W.Yin[38] J.M.You[16] Y.W.Yu[41] N.Yunus[16] M.Yzerman[2] C.Zaccardelli[30] P.Zemp[45] M.Zeng[16] Y.Zeng[1] D.H.Zhang[2] Z.P.Zhang[18,16] B.Zhou[9] G.J.Zhou[6] J.F.Zhou[1] R.Y.Zhu[30] A.Zichichi[7,15,16] B.C.C.van der Zwaan[2]

1 I. Physikalisches Institut, RWTH, W-5100 Aachen, FRG[§]
III. Physikalisches Institut, RWTH, W-5100 Aachen, FRG[§]
2 National Institute for High Energy Physics, NIKHEF, NL-1009 DB Amsterdam, The Netherlands
3 University of Michigan, Ann Arbor, MI 48109, USA
4 Laboratoire d'Annecy-le-Vieux de Physique des Particules, LAPP,IN2P3-CNRS, BP 110, F-74941 Annecy-le-Vieux CEDEX, France
5 Johns Hopkins University, Baltimore, MD 21218, USA
6 Institute of High Energy Physics, IHEP, Beijing, P.R. China
7 INFN-Sezione di Bologna, I-40126 Bologna, Italy
8 Tata Institute of Fundamental Research, Bombay 400 005, India
9 Boston University, Boston, MA 02215, USA
10 Northeastern University, Boston, MA 02115, USA
11 Central Research Institute for Physics of the Hungarian Academy of Sciences, H-1525 Budapest 114, Hungary[‡]
12 Harvard University, Cambridge, MA 02139, USA
13 Massachusetts Institute of Technology, Cambridge, MA 02139, USA
14 INFN Sezione di Firenze and University of Florence, I-50125 Florence, Italy
15 European Laboratory for Particle Physics, CERN, CH-1211 Geneva 23, Switzerland
16 World Laboratory, FBLJA Project, CH-1211 Geneva 23, Switzerland
17 University of Geneva, CH-1211 Geneva 4, Switzerland
18 Chinese University of Science and Technology, USTC, Hefei, Anhui 230 029, P.R. China
19 University of Lausanne, CH-1015 Lausanne, Switzerland
20 Lawrence Livermore National Laboratory, Livermore, CA 94550, USA
21 Los Alamos National Laboratory, Los Alamos, NM 87544, USA
22 Institut de Physique Nucléaire de Lyon, IN2P3-CNRS,Université Claude Bernard, F-69622 Villeurbanne Cedex, France
23 Centro de Investigaciones Energeticas, Medioambientales y Tecnologicas, CIEMAT, E-28040 Madrid, Spain
24 INFN-Sezione di Milano, I-20133 Milan, Italy
25 Institute of Theoretical and Experimental Physics, ITEP, Moscow, Russia
26 INFN-Sezione di Napoli and University of Naples, I-80125 Naples, Italy
27 Department of Natural Sciences, University of Cyprus, Nicosia, Cyprus
28 University of Nymegen and NIKHEF, NL-6525 ED Nymegen, The Netherlands
29 Oak Ridge National Laboratory, Oak Ridge, TN 37831, USA
30 California Institute of Technology, Pasadena, CA 91125, USA
31 INFN-Sezione di Perugia and Universitá Degli Studi di Perugia, I-06100 Perugia, Italy
32 Carnegie Mellon University, Pittsburgh, PA 15213, USA
33 Princeton University, Princeton, NJ 08544, USA
34 INFN-Sezione di Roma and University of Rome, "La Sapienza", I-00185 Rome, Italy
35 Nuclear Physics Institute, St. Petersburg, Russia
36 University of California, San Diego, CA 92182, USA
37 Dept. de Fisica de Particulas Elementales, Univ. de Santiago, E-15706 Santiago de Compostela, Spain
38 Shanghai Institute of Ceramics, SIC, Shanghai, P.R. China
39 Bulgarian Academy of Sciences, Institute of Mechatronics, BU-1113 Sofia, Bulgaria
40 Center for High Energy Physics, Korea Advanced Inst. of Sciences and Technology, 305-701 Taejon, Republic of Korea
41 University of Alabama, Tuscaloosa, AL 35486, USA
42 Purdue University, West Lafayette, IN 47907, USA
43 Paul Scherrer Institut, PSI, CH-5232 Villigen, Switzerland
44 DESY-Institut für Hochenergiephysik, O-1615 Zeuthen, FRG
45 Eidgenössische Technische Hochschule, ETH Zürich, CH-8093 Zürich, Switzerland
46 University of Hamburg, W-2000 Hamburg, FRG
47 High Energy Physics Group, Taiwan, ROC
§ Supported by the German Bundesministerium für Forschung und Technologie
‡ Supported by the Hungarian OTKA fund under contract number 2970.
† Deceased.

# References


[1] L3 Collab., B. Adeva *et al.*, Nucl. Inst. and Meth. **A289** (1990) 35.

[2] L3 Collab., O. Adriani *et al.*, "Experimental Results from L3 at LEP: Electron-Positron Physics at the $Z^0$ Pole", to be published in Physics Report.

[3] L3 Collab., B. Adeva *et al.*, Phys. Lett. **B275** (1992) 209;
L3 Collab., O. Adriani *et al.*, "Determination of the Number of Light Neutrino Species", CERN-PPE/92-128, to be published in Phys. Lett. B.

[4] L3 Collab., B. Adeva *et al.*, Phys. Lett. **B259** (1991) 199;
L3 Collab., O. Adriani *et al.*, Phys. Lett. **B286** (1992) 403.

[5] S. Jadach and B.F.L. Ward, Phys. Lett. **B274** (1992) 470.

[6] D.R. Yennie, S.C. Frautschi and H. Suura, Annals of Physics **13** (1961) 379.

[7] W.J. Stirling, Phys. Lett. **B271** (1991) 261;
S. Jadach *et al.*, Phys. Rev. **D42** (1990) 2977;
S. Jadach, E. Richter-Wąs and B.F.L. Ward, private communication.

[8] The L3 detector simulation is based on GEANT version 3.14,
See R. Brun *et al.*, "GEANT 3", CERN-DD/EE/84-1 (Revised), September, 1987.
The GHEISHA program (H. Fesefeldt, RWTH Aachen Preprint PITHA 85/02 (1985) is used to simulate hadronic interactions.

[9] L3 Collab., O. Adriani *et al.*, "Isolated Hard Photon Emission in Hadronic $Z^0$ Decays", CERN-PPE/92-131, to be published in Phys. Lett. B.

# Figure Captions

Fig. 1 Pictures for the four high mass photon pair events:

(a) Event one: $\mu^+\mu^-\gamma\gamma$, $R-\phi$ view. Starting from the interaction region, the detectors shown in the figure are central tracking chamber, electromagnetic calorimeter, hadron calorimeter, and muon spectrometer.

(b) Event two: $\mu^+\mu^-\gamma\gamma$, $R-\phi$ view;

(c) Event three: $\mu^+\mu^-\gamma\gamma$, $R-z$ view;

(d) Event four: $e^+e^-\gamma\gamma$, $R-z$ view.

Fig. 2 (a) The energy distribution of the most energetic photon for the selected $\ell^+\ell^-$ events with one or more photons in the final state, (b) The energy distribution of the second most energetic photon for the selected $\ell^+\ell^-$ events with at least two photons. The Monte Carlo distributions are obtained from a high statistics sample corresponding to approximately $10^7$ $e^+e^- \to \mu^+\mu^-(n\gamma)$ events generated with YFS3 [5] program. The distributions are normalized to the expected number of $\ell^+\ell^-$ events with one or more photons as shown in Table 2.

Fig. 3 The angle distribution of the most energetic photon with respect to the nearest lepton for the selected $\ell^+\ell^-$ events with at least one photon. The Monte Carlo distribution is obtained from a high statistics sample corresponding to approximately $10^7$ $e^+e^- \to \mu^+\mu^-(n\gamma)$ events generated with YFS3 [5] program. The distribution is normalized to the expected number of $\ell^+\ell^-$ events with at least one photon as shown in Table 2.

Fig. 4 The scatter plot of $M_{\gamma\gamma}$ versus $M_{\ell\ell}$ for $\ell^+\ell^-$ events with two or more photons for the data (a) and for the Monte Carlo after detector simulation (b). The data plot is obtained from a sample of 48,587 selected $\ell^+\ell^-(n\gamma)$ events while the Monte Carlo distribution is obtained from a sample of 84,633 selected $\mu^+\mu^-(n\gamma)$ events. The Monte Carlo events are generated with YFS3 [5] program.

Fig. 5 The distribution of $M_{\gamma\gamma}$ versus $\cos\theta_{\gamma\ell}$ for the selected $\ell^+\ell^-$ events with two or more photons for the data (a) and the fully simulated Monte Carlo (b). The data plot is obtained from a sample of 48,587 selected $\ell^+\ell^-(n\gamma)$ events while the Monte Carlo distribution is obtained from a sample of 84,633 selected $\mu^+\mu^-(n\gamma)$ events. The Monte Carlo events are generated with YFS3 [5] program.

Fig. 6 $M_{\gamma\gamma}$ distribution of the data for $\ell^+\ell^-$ events with two or more photons compared to the expectation from the Monte Carlo. The Monte Carlo distribution is obtained from a high statistics sample corresponding to approximately $10^7$ $e^+e^- \to \mu^+\mu^-(n\gamma)$ events generated with YFS3 [5] program. The distribution is normalized to the expected number of $\ell^+\ell^-$ events with at least two photons as shown in Table 2.

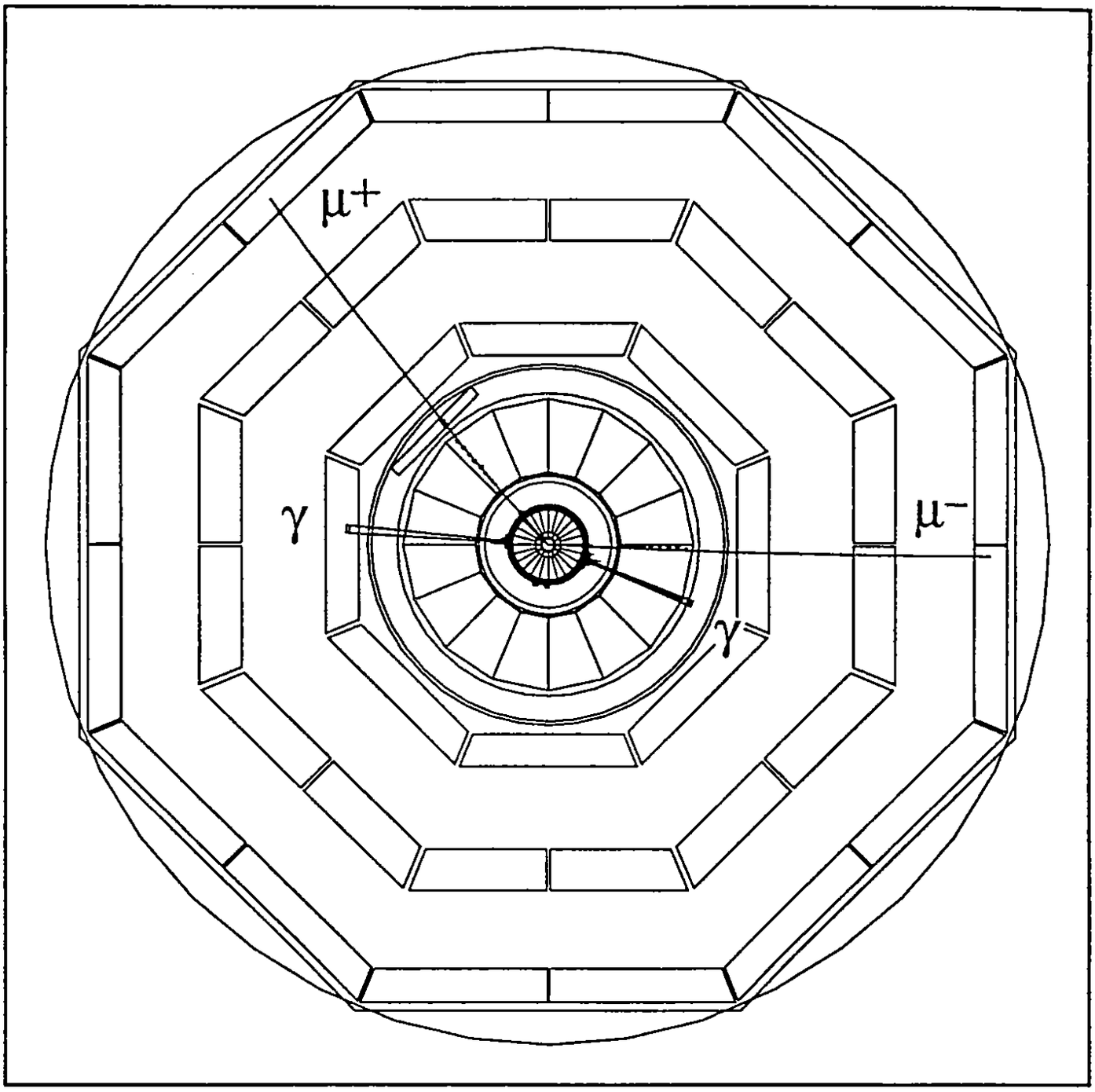


**Figure 1a**

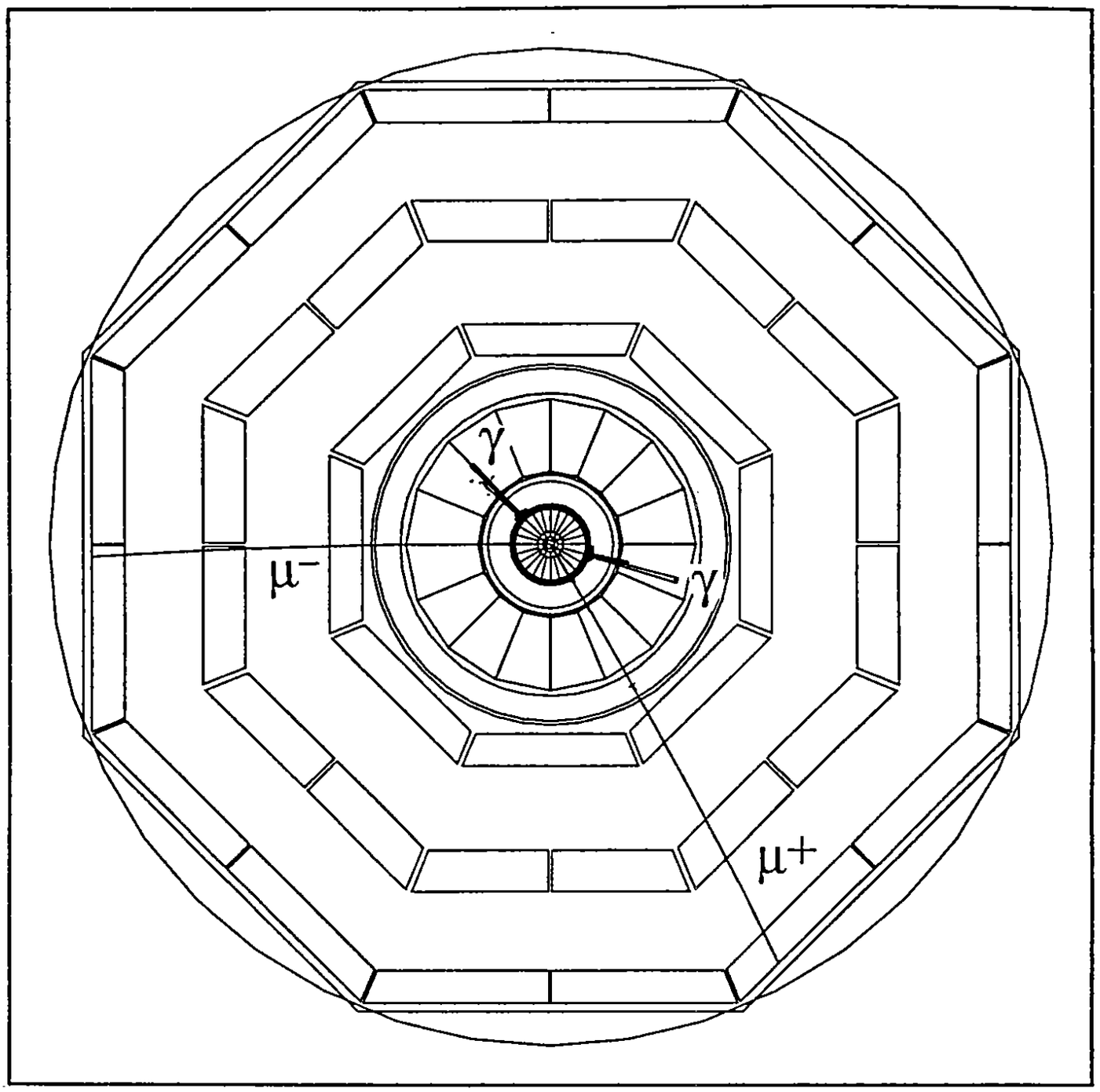


**Figure 1b**

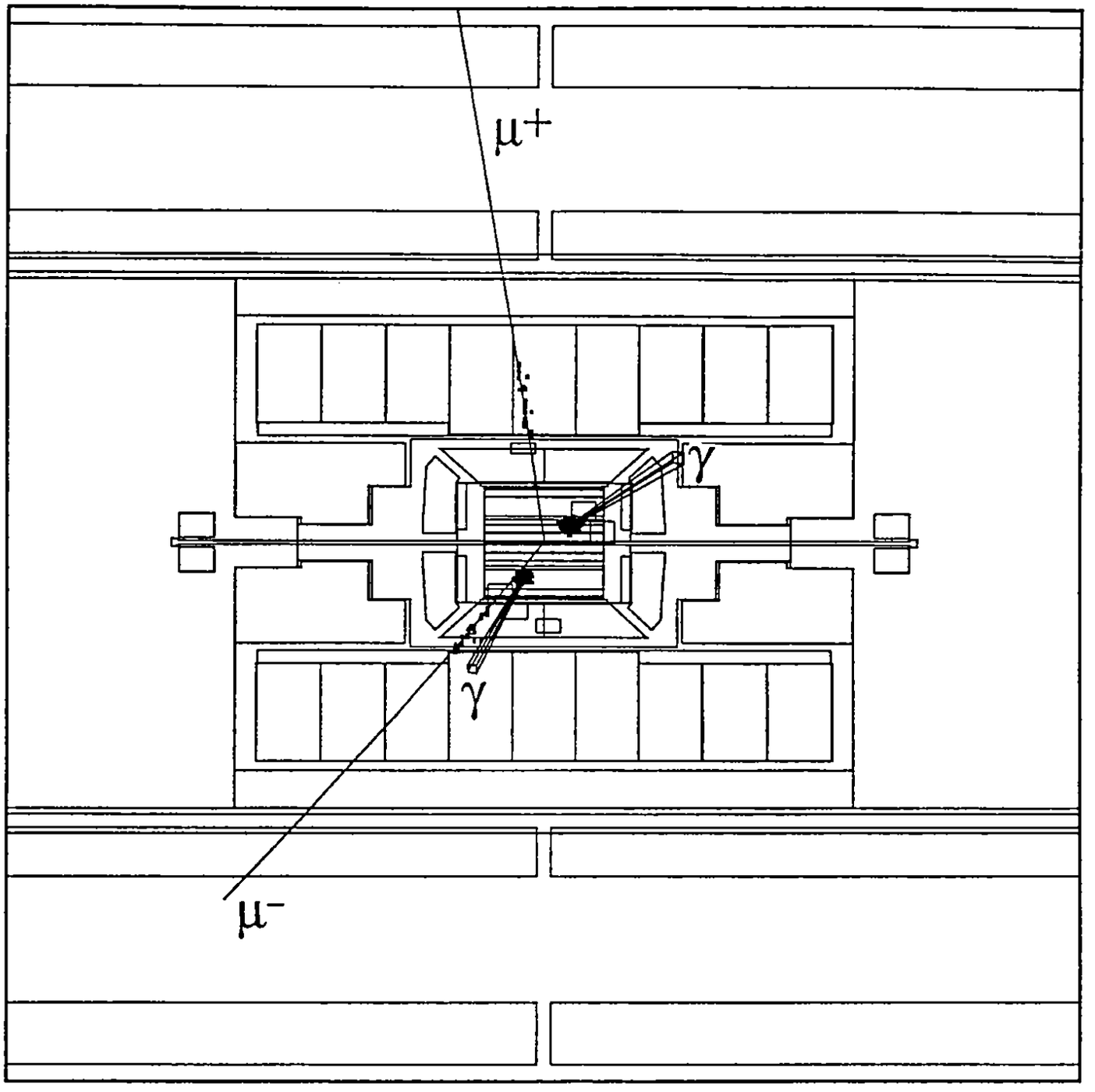


**Figure 1c**

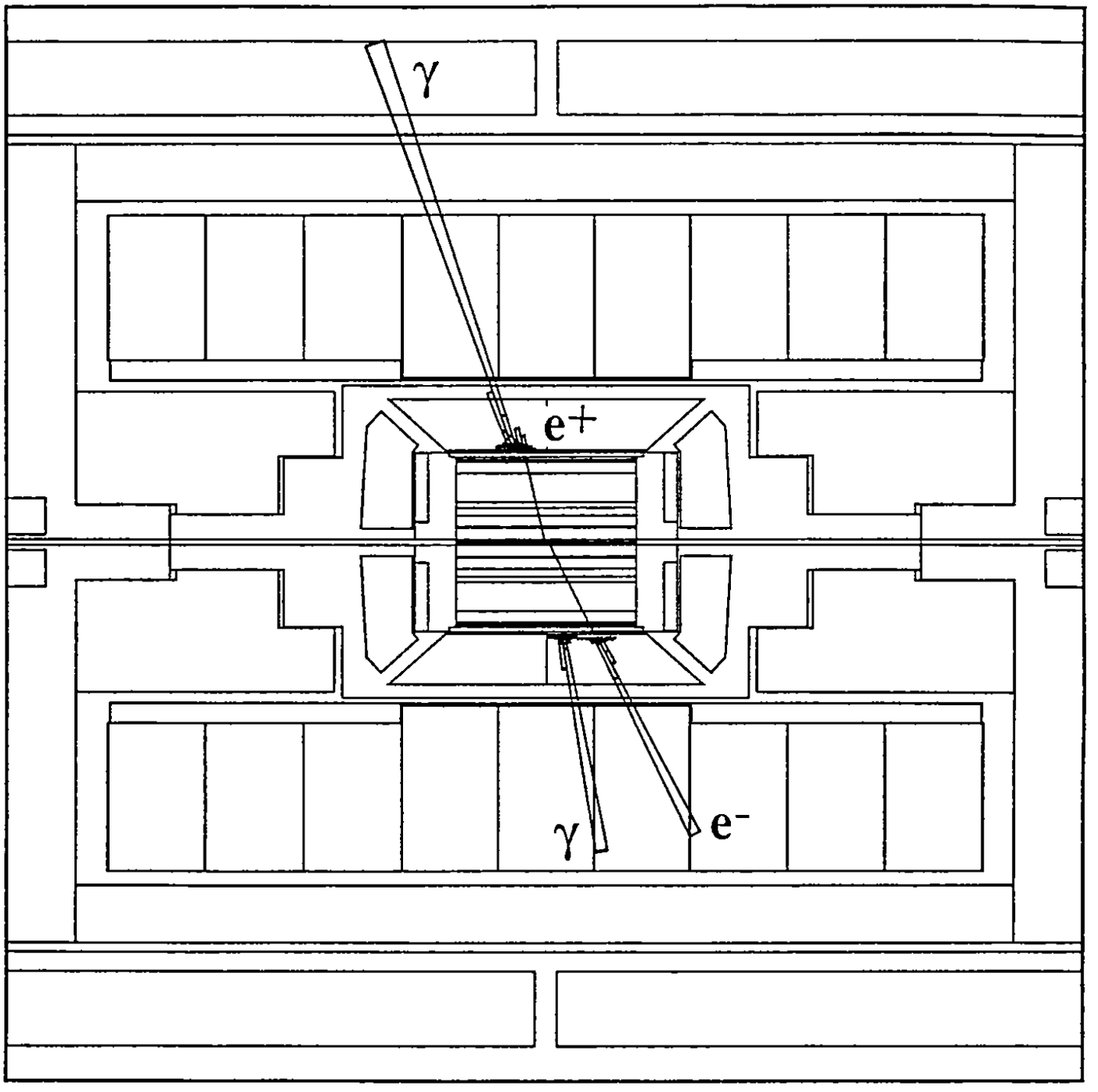


**Figure 1d**

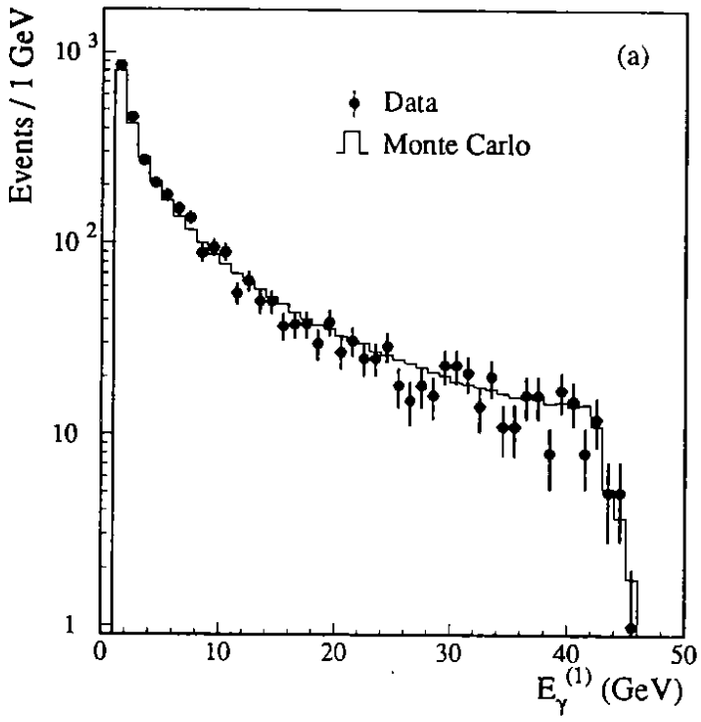
(a)
Data
Monte Carlo
Events / 1 GeV
$10^3$
$10^2$
10
1
0
10
20
30
40
50
$E_\gamma^{(1)}$ (GeV)

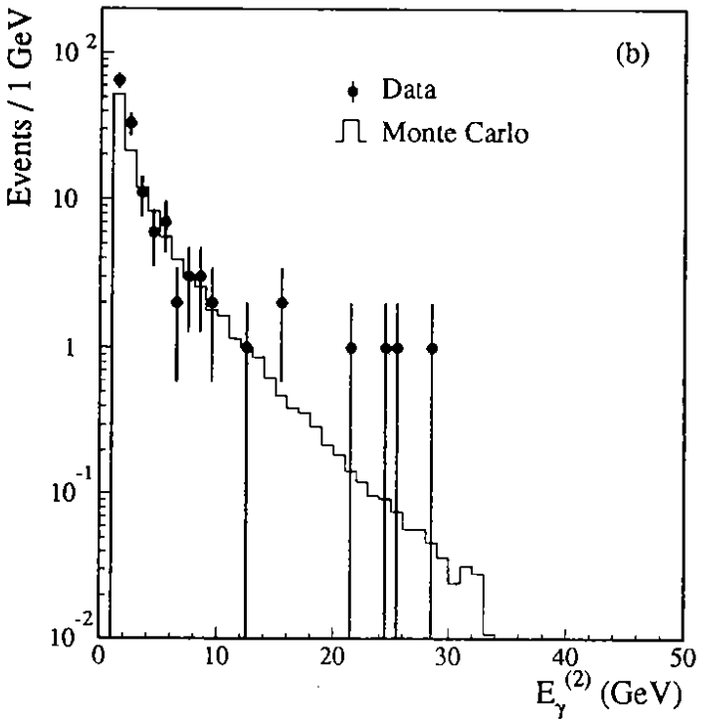
(b)
Data
Monte Carlo
Events / 1 GeV
$10^2$
10
1
$10^{-1}$
$10^{-2}$
0
10
20
30
40
50
$E_\gamma^{(2)}$ (GeV)

# Figure 2

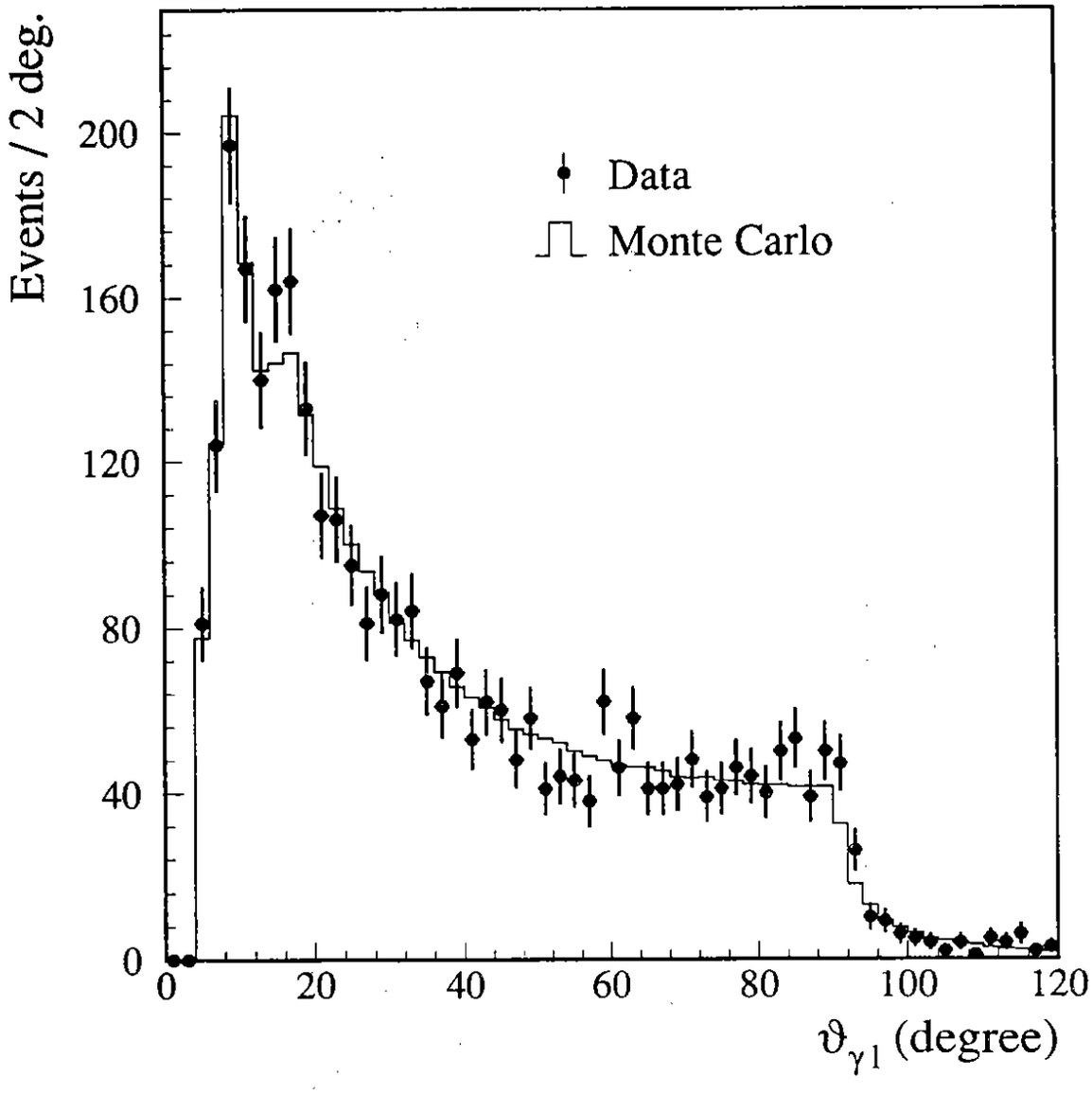
Events / 2 deg.
200
160
120
80
40
0
0
20
40
60
80
100
120
Data
Monte Carlo
$\vartheta_{\gamma 1}$ (degree)

**Figure 3**

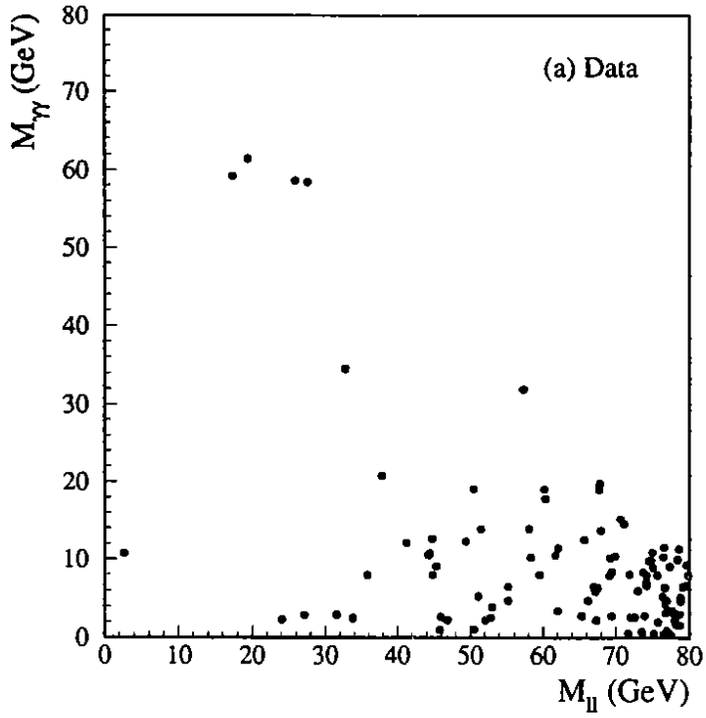
(a) Data
$M_{\gamma\gamma}$ (GeV)
$M_{ll}$ (GeV)
0
10
20
30
40
50
60
70
80

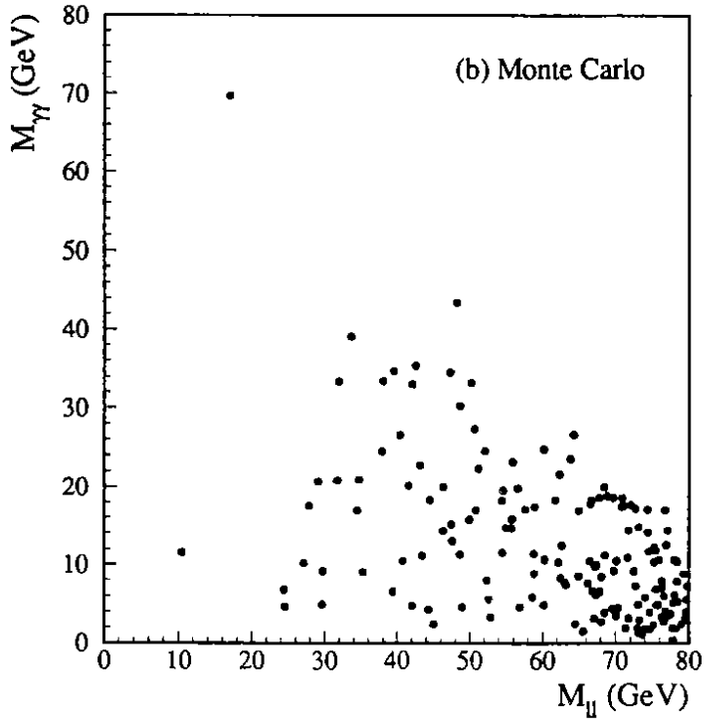
(b) Monte Carlo
$M_{\gamma\gamma}$ (GeV)
$M_{ll}$ (GeV)
0
10
20
30
40
50
60
70
80

# Figure 4

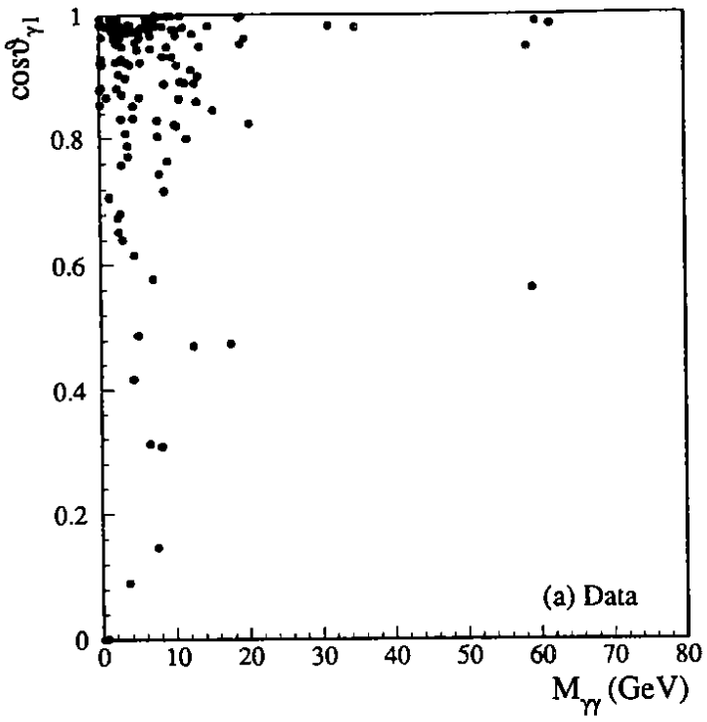
cosϑγ1
1
0.8
0.6
0.4
0.2
0
0
10
20
30
40
50
60
70
80
Mγγ (GeV)
(a) Data

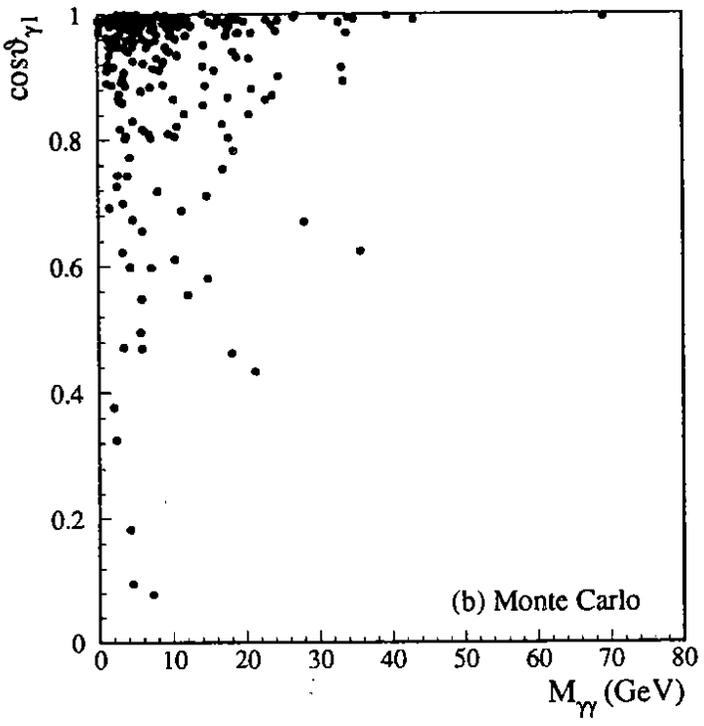
cosϑγ1
1
0.8
0.6
0.4
0.2
0
0
10
20
30
40
50
60
70
80
Mγγ (GeV)
(b) Monte Carlo

# Figure 5

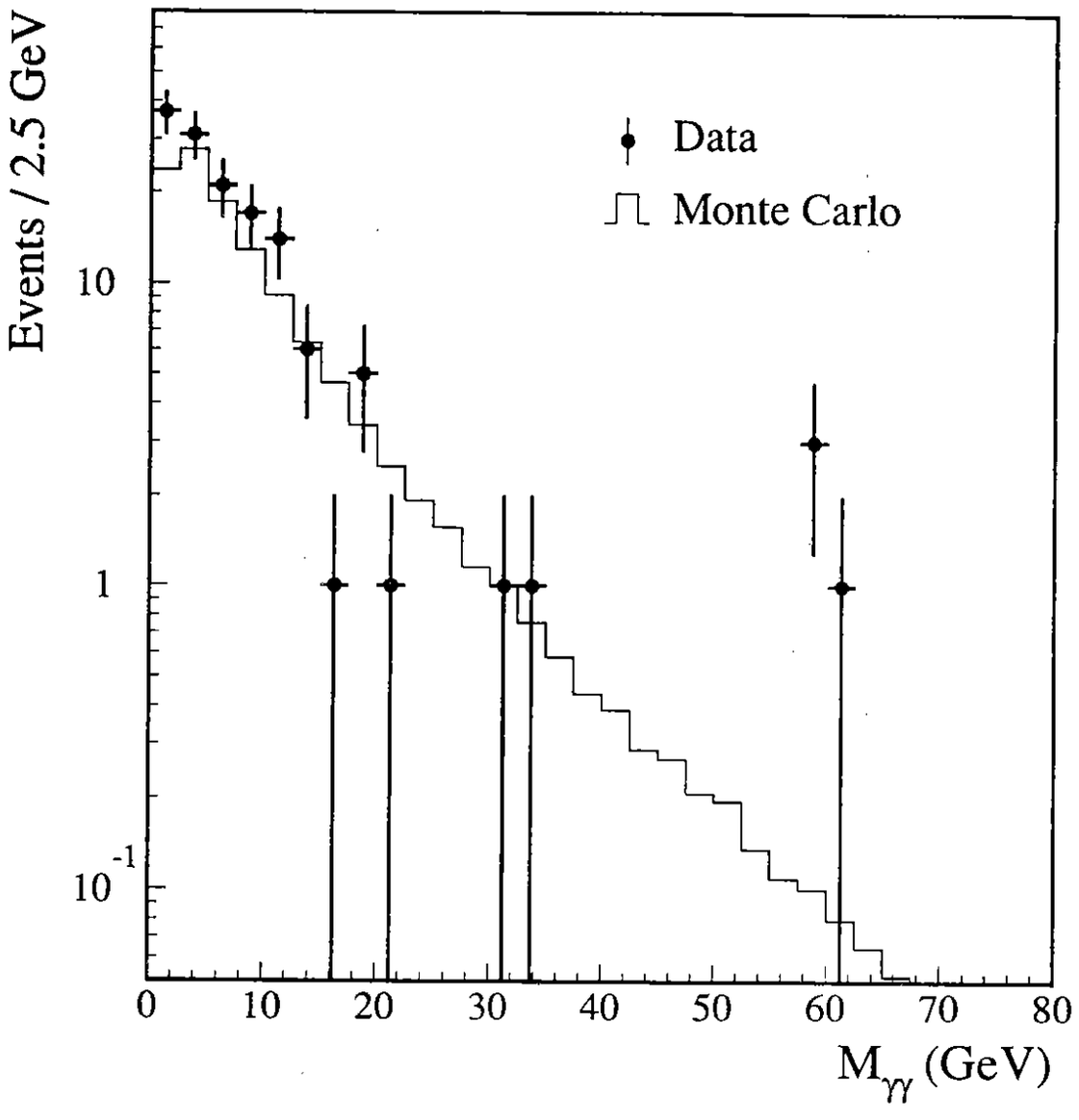
Events / 2.5 GeV
Data
Monte Carlo
10
1
$10^{-1}$
0
10
20
30
40
50
60
70
80
$M_{\gamma\gamma}$ (GeV)

**Figure 6**